Regular Linking of Cellulose Nanocrystals via Click Chemistry: Synthesis and Formation of Cellulose Nanoplatelet Gels

Ilari Filpponen[†] and Dimitris S. Argyropoulos[*,†,‡]

Organic Chemistry of Wood Components Laboratory, Department of Forest Biomaterials, North Carolina State University, Raleigh, North Carolina 27695-8005, and Laboratory of Organic Chemistry, Department of Chemistry, University of Helsinki, P.O. Box 55, 00014, Helsinki, Finland

Received January 8, 2010; Revised Manuscript Received February 19, 2010

Over a number of years work in our laboratory has been developing new chemistry for the use of cellulose nanocrystals (CNCs) as scaffolds for the creation of nanomaterials with novel, stimuli responsive characteristics. Our work takes advantage of the rigid nature of CNCs, the unique nanopattern etched on their surface in the form of regularly spaced primary OH groups, and the fact that these materials have all reducing end groups located on one end. In this communication, a method for the grafting of amine-terminated monomers onto surface-modified CNCs followed by click chemistry is demonstrated. Initially the primary hydroxyl groups on the surface of the CNCs were selectively activated by converting them to carboxylic acids by the use of TEMPO-mediated hypohalite oxidation. Further reactions using the activated TEMPO-oxidized CNCs were carried out via carbodiimide-mediated formation of an amide linkage between precursors carrying an amine functionality and the carboxylic acid groups on the surface of the TEMPO-oxidized CNCs. Subsequently, two sets of CNCs were prepared, containing on their surface an azide derivative and an alkyne derivative, respectively. Finally, the click chemistry reaction, that is, the Cu(I)-catalyzed Huisgen 1,3-dipolar cycloaddition between the azide and the alkyne, surface-activated CNC was employed, bringing together the nanocrystalline materials in a unique regularly packed arrangement demonstrating a degree of molecular control for creating these structures at the nano level.

Introduction

The modification of polysaccharides plays a central role in the field of sustainable chemistry.[1] By virtue of their large abundancy and their structural and superstructural diversity, polysaccharides are ideal starting materials for defined modifications and specific applications. The chemical modification of polysaccharides provides a versatile route for structural and property design of such materials.[2] Due to the chemical functionality of polysaccharides (bearing hydroxyl and/or carboxylic acid groups), esterification and etherification are the most common approaches for modification reactions of polysaccharides. Moreover, oxidation and homogeneous nucleophilic substitution reactions are applied but to a lesser extent. Cellulose and dextran are the most commonly used starting materials for the creation of highly engineered nanoparticles.[3–6]

In general, 1,3-dipolar cycloaddition reactions have long been popular in the generation of carbohydrate mimetics in a homogeneous reaction environment.[7] More precisely, the thermally induced cycloaddition (Huisgen reaction) occurs between an azide and a triple bond and is nowadays often referred as a member of the click-reaction family because of its robustness.[8] The reaction has gained increasing attention after discovering that the 1,3-dipolar cycloaddition between azides and terminal alkynes can be catalyzed by Cu(I) salts.[9–14] In fact, the Huisgen reaction has become the most popular click reaction to date by virtue of its high yields, rapidity, high regio- and stereoselectivity, mild reaction conditions, and experimental simplicity. Several authors have described the use of this novel click-chemistry concept for the generation of carbohydrate mimetics and derivatives.[10,15–18]

In 1994, De Nooy et al. reported that the primary alcohol groups of carbohydrates can be selectively oxidized in aqueous media by using the 2,2,6,6-tetramethyl-1-piperidinyloxy (TEMPO) radical.[19] Since then, the technique has been applied with success to various cellulose samples.[20–24] During the course of these investigations it was found that regenerated cellulose could be completely converted into water-soluble polyglucuronic acid, whereas in the case of native cellulose fibers, the oxidation proceeded throughout the fibers but occurred only at the surface of the microfibrils, which therefore became negatively charged. As such, the TEMPO-mediated oxidation is an alternate way to form stable colloidal suspensions of CNCs without having the lability of the sulfate ester groups.

In 2001, Araki and co-workers demonstrated a method for grafting amine-terminated poly(ethylene glycol) to surface-modified (TEMPO-oxidized) cellulose microcrystals, thus, improving the stability of the microcrystal suspensions through steric stabilization.[25] In 2007, Crescenzi et al. extended Araki's approach by modifying hyaluronic acid with the alkyne and azido groups to achieve suitable precursor for the 1,3-dipolar cycloaddition reaction.[26] They modified hyaluronic acid with the alkyne and azido groups to achieve suitable precursor for the 1,3-dipolar cycloaddition reaction.[9,15,16,27–29] Once these precursors were mixed in the aqueous media substantial gel formation was observed. Recently, similar methodology has been successfully applied for cellulose modifications in heterogeneous media.[30,31]

In this paper we describe the formation of nanoplatelet gel-like nanomaterials formed using cellulose nanocrystals (CNC) as the starting material. Initially, the primary hydroxyl groups on the surfaces of the CNCs were selectively activated to carboxylic acids by using TEMPO-mediated hypohalite oxidation. In the next step, compounds carrying terminal amine functionality were grafted on to the surface activated oxidized

* To whom correspondence should be addressed. Tel.: (919) 515-7708. Fax: (919) 515-6302. E-mail: dsargyro@ncsu.edu.
[†] North Carolina State University.
[‡] University of Helsinki.

10.1021/bm1000247
Published on Web 03/17/2010

Scheme 1. Schematic Representation of the Reaction between Cellulose Nanocrystals (CNCs) and 11-Azido-3,6,9-trioxaundecan-1-amine (AZ)

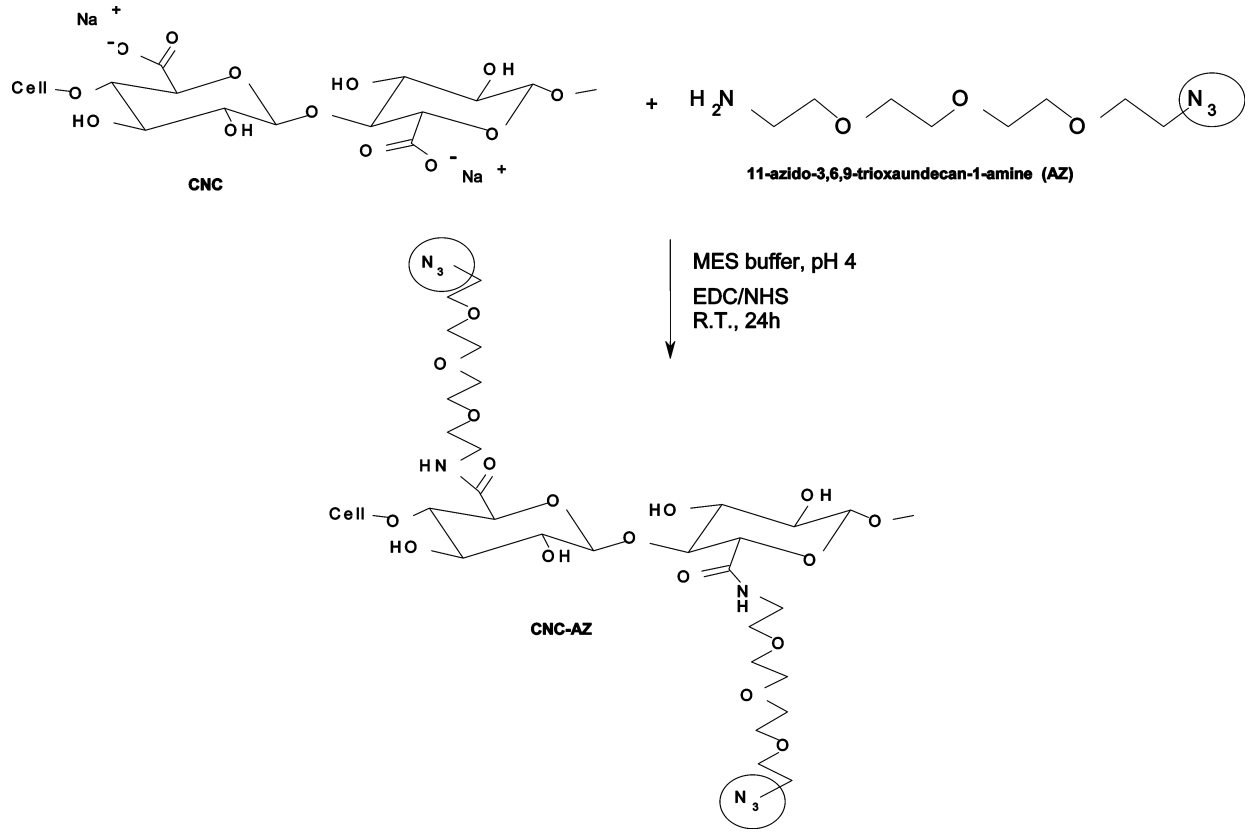

CNCs via the carbodiimide-mediation, creating an amide linkage between the amine and the carboxylic groups on the CNCs surfaces. The grafted amine compounds contained terminal alkyne or azide functionalities and as such two sets of precursors were prepared. The alkyne and azide, surface-functionalized CNC precursors, were then brought together via click chemistry, creating for the first time unique nanoplatelet gels, as evidenced by detailed transmission electron microscopic investigations (TEM).

Materials and Methods

Materials. Whatman #1 filter paper was used as a starting material for the cellulose nanocrystals. 11-Azido-3,6,9-trioxaundecan-1-amine (technical, ≥90%) was purchased from Fluka and propargylamine (98%) from Sigma-Aldrich. All other chemicals were purchased from Sigma-Aldrich or Fisher and used as received unless otherwise stated.

Methods. *Acid Hydrolysis of Cellulose To Produce Cellulose Nanocrystals (CNC).* The cellulose nanocrystals were formed by acidic hydrolysis similar to the procedure used by Araki et al.[25,32,33] A typical procedure was as follows: 2.0 g of cellulose pulp obtained from Whatman #1 filter paper (98% α-cellulose, 80% crystallinity) was blended by a 10 Speed Osterizer Blender. The resulting pulp was hydrolyzed with 100 mL of 2.5 M HBr at 100 °C for 3 h. The ultrasonication was applied during (every 60 min) the reaction (Omni-Ruptor 250W ultrasonic homogenizer, 50% power, 5 min). The resulting mixture was diluted with deionized (D.I.) water followed by five cycles of centrifugation at 1500 g for 10 min (IEC Centra-CL3 Series) to remove excess acid and water-soluble fragments. The fine cellulose particles became dispersed in the aqueous solution approximately at pH 4. The turbid supernatant containing the polydisperse cellulose particles was then collected for further centrifugation at 15000 g for 45 min (Automatic Servall Superspeed Centrifuge) to remove ultrafine particles. Ultrafine particles with small aspect ratio were removed from the upper layer, and the precipitation (after the high-speed centrifugation) was dried using a lyophilizing system (Labconco, Kansas City, MU).

TEMPO-Mediated Oxidation of CNCs. A total of 648 mg (4 mmol of glucosyl units) of cellulose nanocrystals were suspended in water (50 mL) containing 10 mg of 2,2,6,6-tetramethyl-1-piperidinyloxy-radical (TEMPO, 0.065 mmol) and 200 mg of sodium bromide (1.9 mmol) at room temperature for 30 min. The TEMPO-mediated oxidation of the cellulose nanocrystals was initiated by slowly adding 4.90 mL of 13% NaClO (8.6 mmol) over 20 min at room temperature under gentle agitation. The reaction pH was monitored using a pH meter and maintained at 10 by incrementally adding 0.5 M NaOH. When no more decrease in pH was observed, the reaction was considered complete. About 5 mL of methanol was then added to react and quench with the extra oxidant. After adjusting the pH to 7 by adding 0.5 M HCl, the TEMPO-oxidized product was washed with D.I. water by centrifugation and further purified by dialysis against D.I. water for two days. A total of 550 mg of solid was recovered after freeze-drying. FTIR measurements showed a carboxylic acid peak at 1730 cm^{-1}. The carboxylic content in the oxidized cellulose nanocrystals was determined by FTIR and NaOH titration.

Synthesis of Click Precursor Bearing Azide Groups (CNC-AZ). A 50 mg amount of TEMPO-oxidized CNCs were mixed in 6 mL of MES [2-(*N*-morpholino)-ethanesulfonic acid buffer (50 mM, pH = 4)]. The resulting suspension was further treated with ultrasound treatment (5 min, 20% power (50W) with 30% pulser on; Omni-Ruptor 250 Ultrasonic Homogenizer, Omni International Inc.) to break down the cellulose aggregates. In a typical synthesis, 120 mg EDC·HCl [*N*-(3-dimethylaminopropyl)-*N*′-ethylcarbodiimide hydrochloride)], 72 mg NHS (*N*-hydroxysuccinimide), and 200 μL of 11-azido-3,6,9-trioxaundecan-1-amine, respectively, were added to the CNC suspension. The reaction was performed at room temperature under stirring for 24 h. The resulting mixture was dialyzed (cutoff = 12 kDa) against aqueous

Scheme 2. Schematic Representation of the Reaction between Cellulose Nanocrystals (CNCs) and Propargylamine (PR)

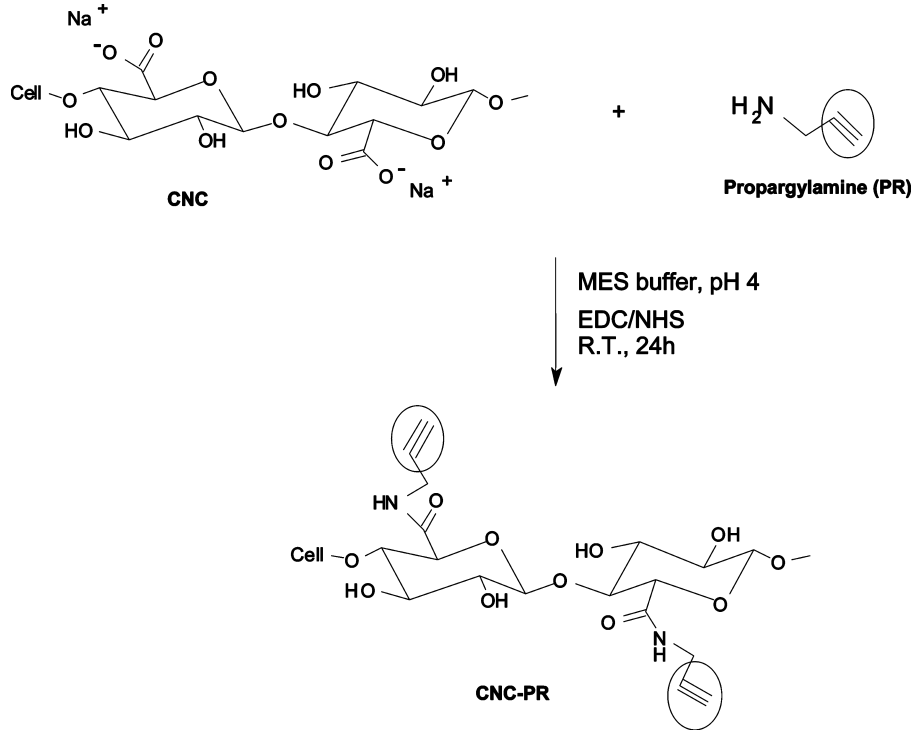

saturated NaCl for 1 day and then against distilled water for 3 days. Finally, the solutions were dried using a lyophilizing system to recover the CNC-AZ derivatives (see Scheme 1).

Synthesis of Click Precursor Bearing Alkyne Groups (CNC-PR). TEMPO-oxidized CNCs (50 mg) were mixed in 6 mL of MES [2-(*N*-morpholino)-ethanesulfonic acid buffer (50 mM, pH = 4)]. The resulting suspension was further treated with ultrasound treatment (5 min, 20% power with 30% pulser on; Omni-Ruptor 250 Ultrasonic Homogenizer, Omni International Inc.) to break down the cellulose aggregates. In a typical synthesis, 120 mg EDC·HCl [*N*-(3-dimethylaminopropyl)-*N*′-ethylcarbodiimide hydrochloride)], 72 mg NHS (*N*-hydroxysuccinimide), and 60 μL of propargylamine, respectively, were added to the CNC suspension. The reaction was performed at room temperature under stirring for 24 h. The resulting mixture was dialyzed (cutoff = 12 kDa) against a saturated NaCl solution for 1 day and then against distilled water for 3 days. Finally, the CNC-PR derivatives (see Scheme 2) were recovered by freeze-drying.

Synthesis of Click Product (CNC-Click). A 25 mg amount of CNC-AZ and 25 mg CNC-PR were mixed in 3.0 mL of distilled water. Next, 25 μL of $CuSO_4 \cdot 5H_2O$ aqueous solution (7.5% w/v) and 30 μL of ascorbic acid (1 M sol.) were added, and the mixture was vigorously stirred, leading to a formation of a stable gel (click gel: Scheme 3). The gel was left at rest overnight and then dialyzed against EDTA solution (10 mM) for 12 h and finally against distilled water until constant weight.

Benzoylation of Click Precursors and Click Product. The method described below was developed by the group of Argyropoulos following the principles established in the work described elsewhere.[34] Ionic liquid, 1-allyl-3-methylimidazolium chloride ([Amim]Cl, 950 mg), was added to CNC (50 mg) in a 15 mL sample flask, vortexed until all solid particles had dispersed, and heated at 80 °C with magnetic stirring until the solutions were transparent (2 h). Pyridine (330 μL, 3.7 mmol) was added and the solution was vortexed until homogeneous and allowed to cool down to room temperature. Benzoyl chloride (380 μL, 3.3 mmol) was added in one portion, and the resulting mixture was vortexed until the formation of homogeneous white paste. The sample was then heated at 55 °C for 3 h with magnetic stirring and then allowed to cool down to the room temperature. Next, the mixture of deionized water (2.5 mL) and EtOH (7.5 mL) was added and the mixture was vigorously shaken and vortexed for 5 min. The solid was filtered off through a sintered funnel (grade M), washed further with EtOH, and purified with MeOH (stirred overnight without heating). Finally, the resulting solid was filtered off to give a white powder (84 mg).

Infrared Spectroscopy. FTIR spectra were measured on a Thermo Nicolet NEXUS 670 FT-IR infrared spectrophotometer. Spectra in the range of 4000−650 cm^{-1} were obtained with a resolution of 4 cm^{-1} by cumulating 64 scans. Degree of oxidation (DO) measurements were carried out by comparing the intensities of absorption band near 1730 cm^{-1} (carbonyl stretching frequency) to that of 1050 cm^{-1} (cellulose backbone).[35]

Acid−Base Titration. The carboxylic acid content of the oxidized CNCs was determined by acid−base titration following the procedure developed for the conductometric titrations of such materials.[36] In this procedure TEMPO-oxidized CNC samples (50 mg) were suspended into 0.01 M hydrochloric acid (HCl) solutions (15 mL) with stirring. The resulting suspensions were then titrated with 0.01 M sodium hydroxide (NaOH) solution. The degree of oxidation (DO) values were calculated as already published, and very reproducible results were obtained.[36]

Elemental Analysis. The percent carbon (C), hydrogen (H), and nitrogen (N) contents (%) of the unreacted TEMPO-oxidized cellulose nanocrystals, its alkyne and azido derivatives, and click product were determined by Perkin-Elmer element analyzer (Norwalk, CT). The remaining sample was assumed to be oxygen (O).

Thermal Analysis. Thermal decomposition temperatures were determined using a TA Instrument TGAQ500 at a ramp of 10 °C/min under N_2 purge.

Transmission Electron Microscopy. Suspensions (0.01% w/v in water) of unmodified cellulose nanocrystal, TEMPO-oxidized cellulose nanocrystals, and cellulose nanocrystals after the click reaction were prepared. Drops of each suspension were deposited on carbon-coated electron microscope grids, negatively stained with uranyl acetate and allowed to dry. The grids were observed with a Hitachi HF2000 microscope (FEI Company, U.S.A.) operated at an accelerating voltage of 200 kV.

GPC Analysis. Gel permeation chromatographic (GPC) measurements were carried out with a Waters GPC 510 pump equipped with

Scheme 3. Schematic Representation of the Formation of CNC-Based Nanoplatelet Gels

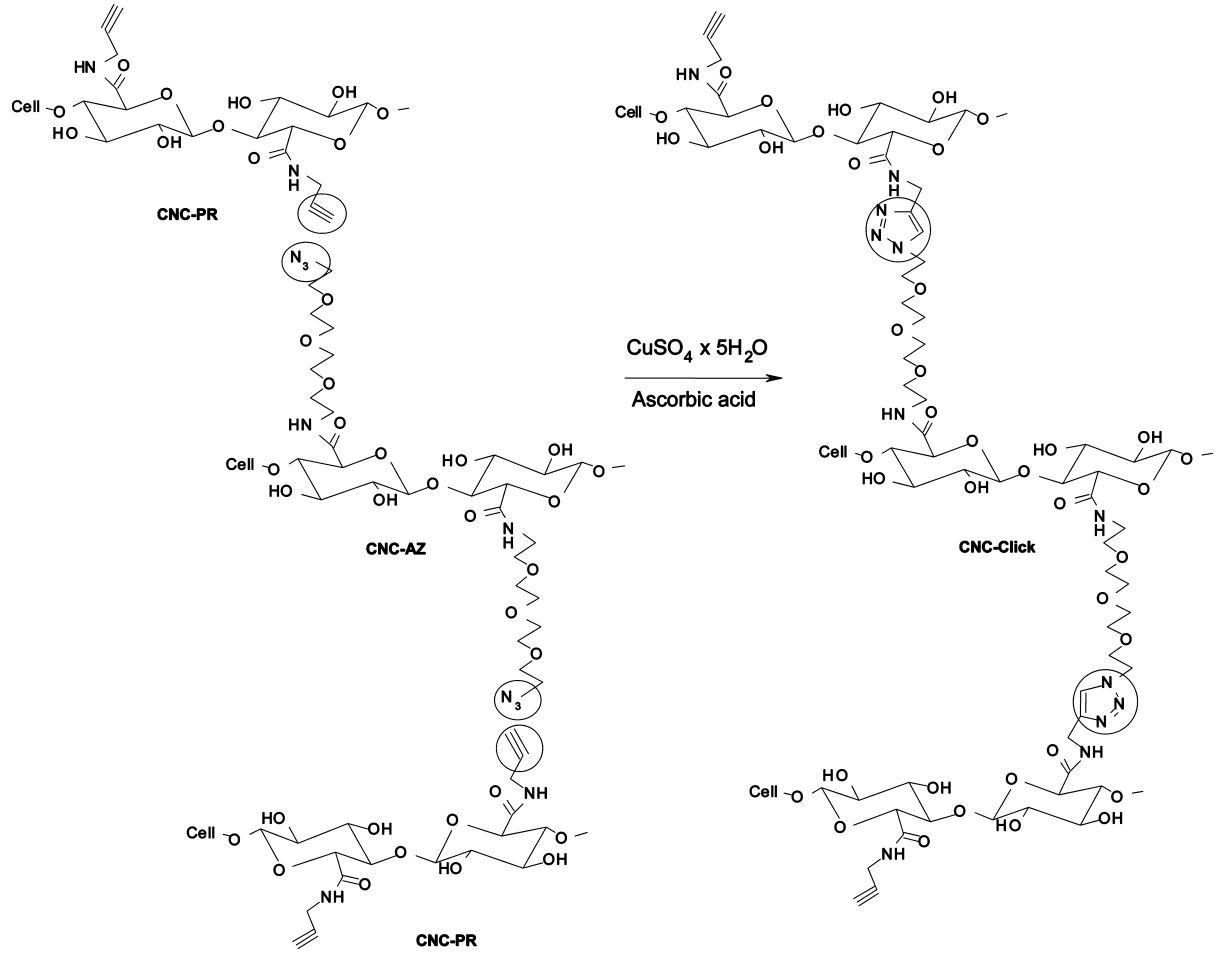

UV and RI detectors using THF as the eluent at a flow rate of 0.7 mL/min at 40 °C. Two Ultrastyragel linear columns (Styragel HR 1 and Styragel HR 5E), connected in series, were used for the measurements. Standard polystyrenes of narrow dispersity with molecular weight ranges from 0.82 to 1860 kg/mol were used for calibration. The number- and weight-average molecular weights were calculated using the Millenium software of Waters.

Results and Discussion

TEMPO-Mediated Oxidation of Cellulose Nanocrystals. TEMPO-oxidation selectively oxidizes the primary hydroxyl groups while leaving unaffected the secondary hydroxyl groups.[21,36] With proper reaction conditions, TEMPO-oxidation can be controlled only occurring on the surface of native cellulose crystalline.[22,37] Due to the cellulose molecule's packing fashion, one-half of the primary hydroxyl (hydroxymethyl) groups on the surface cellulose chains point toward the core of the crystalline domain and are, thus, inaccessible to the oxidation. Based on the arrangement of the cellulose molecule in the crystalline unit cell,[38] the carboxylic groups created on the nanocrystal surface should be 1.0 nm apart in the longitudinal direction and 0.8 nm apart in the width direction. This is a unique feature of cellulose nanocrystals. As such, our work aims at taking advantage of this etched nanopattern on the surface of these materials. More specifically, our work aims at the careful and selective activation of the primary OH groups, coupled with further chemical manipulations for the creation of materials controlled at the nanolevel. The introduction, therefore, of carboxyl groups on the surface of the cellulose nanocrystals at a regularly spaced nanopattern without destroying the crystalline arrangement of these nanomaterials represents a major initial step toward fulfilling our ultimate objectives.

Chemical Characterization of Oxidized Cellulose Nanocrystals. The cotton cellulose crystals are of a rectangular shape with average dimensions of 40 ± 18 Å.[39] Thus, the amount of individual cellulose chains within a cotton crystallite can be calculated using the two lattice parameters of cellulose I_β unit cell, $a = 0.801$ nm and $b = 0.817$ nm, respectively. This model corresponds to a minimum of 4 × 4 and a maximum of 8 × 8 packing (using 40 ± 18 Å as the dimensions) of cellulose chains within a crystallite. Therefore, either 12 of the 16 chains or 28 of the 64 chains present on the surfaces of the crystallite are susceptible to the oxidation. Consequently, the ratio of surface chains to the total number of chains within the crystals is 0.75 or 0.44, that is, 75 or 44% of the cellulose chains can be oxidized, respectively. However, due to the 2-fold screw axis of the cellulose chain only half of the hydroxymethyl groups are accessible to oxidation, the other half is pointing toward the core of the crystalline domain. Therefore, the corresponding degrees of oxidation (DO) that can be achieved for the cotton nanocrystals are 0.75/2 = 0.375 or 0.44/2 = 0.22. However, using the average dimension of 40 Å for a cotton crystallite leads to the DO value of 0.28.

The carboxyl content of oxidized cellulose samples was determined by acid−base titrations and FTIR, as described in Materials and Methods. The titration curves showed the presence of strong acid, corresponding with the excess of HCl and weak acid corresponding to the carboxyl content, as shown in Figure

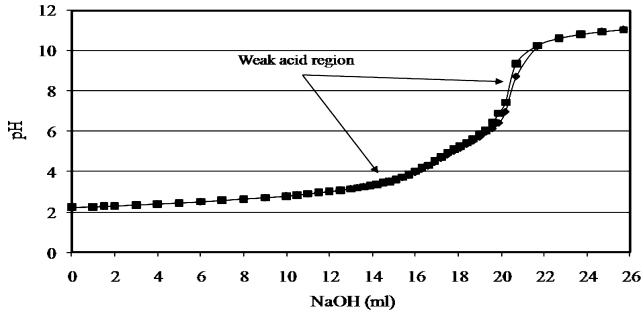

Figure 1. Titration curves of the oxidized (TEMPO) cellulose nanocrystals.

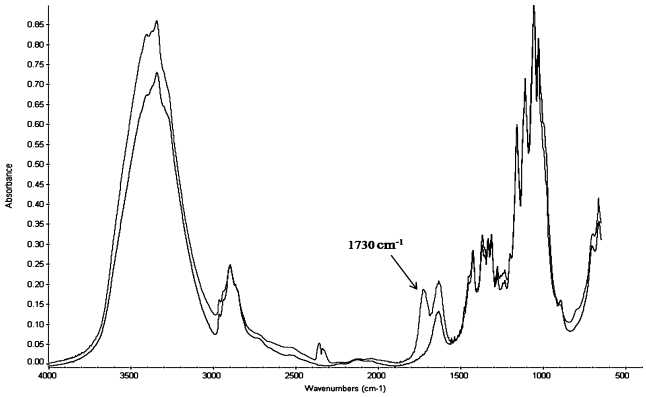

Figure 2. FTIR spectrum of cellulose nanocrystals (lower) and TEMPO-oxidized cellulose nanocrystals (upper).

1. In the first step of titration, NaOH neutralizes the added excess hydrochloric acid (strong acid), which is then followed by the neutralization of the carboxylic acid groups (weak acid). The amount of NaOH needed for the neutralization of the carboxylic acid groups was determined as the difference between the known amount (15 mL) of NaOH consumed for the neutralization of HCl and the equivalence point of the weak acid titration of carboxylic acid groups. As can been seen from the Figure 1, the equivalence point appears at pH 8.0 subsequent to the overall NaOH consumption of 20.5 mL. Thus, the neutralization of the carboxylic acid groups consumes 5.5 mL of NaOH (20.5−15.0 mL), corresponding to the DO value of 0.19.[36]

FTIR spectra of TEMPO-oxidized cellulose nanocrystals is seen to contain a new band at around 1730 cm^{-1} when compared to the starting cellulose nanocrystals (Figure 2). The new band corresponds to the C═O stretching frequency of carboxyl groups in their acidic forms. The DO values can be roughly estimated by comparing the intensity of the new band at 1730 cm^{-1} to that near 1050 cm^{-1} which is derived from the cellulose backbone.[35] For example, the corresponding band intensities in Figure 2 are 0.2 and 0.95 leading to a DO value of 0.21 (0.2/0.95). At this point it can be concluded that the DO values obtained from acid−base titration and FTIR are in good agreement.

FTIR Analysis of the TEMPO-Oxidized CNCs and Click Derivatives. The click reaction of the CNC derivatives was followed by FTIR measurements. Figure 3a clearly displays the carbonyl stretching band at 1730 cm^{-1} for the TEMPO-oxidized CNCs. This band is seen to be eliminated during the formation of the azide derivative (CNC-AZ), which in turn has a characteristic azide stretching band at about 2110 cm^{-1} (Figure 3b). The disappearance of the carbonyl stretching band is due to the formation of the amide linkages between the TEMPO-oxidized CNCs and amine-bearing precursor molecules. The amides, on the other hand, are known to have a characteristic stretching band at around 1650 cm^{-1}, and as such, the overlapping with the absorbed water band (1640 cm^{-1}) is unavoidable. Furthermore, the azide stretching band is not apparent in the FTIR spectrum of the CNC-Click (Figure 3c), pointing to the successful 1,3-dipolar cycloaddition reaction between the CNC-AZ and CNC-PR.

Elemental Analysis of TEMPO-Oxidized CNCs and Click Derivatives. The nitrogen contents in both click precursors confirmed the successful grafting reactions (Table 1). To eliminate the possible contribution to the product's nitrogen content arising from the cross-linking agents (1-ethyl-3-[3-dimethylaminopropyl]carbodiimide hydrochloride and *N*-hydroxysulfosuccinimide), the TEMPO-oxidized CNCs were subjected to identical reaction conditions in the absence of the derivatization compounds (11-azido-3,6,9-trioxaundecan-1-amine and propargylamine). The nitrogen contents for both of the precursors (CNC-PR and CNC-AZ) as well as for the CNC-Click were found to be higher than that of the starting material. This data was rather valuable in determining the grafting density of the precursors, which ultimately determine the uniformity of the chemistry aimed to be created on the crystals and between adjacent crystals.

The grafting densities of synthesized precursors were calculated based on the DO value (0.2) of the oxidized CNCs determined by FTIR and acid−base titration. The DO value of 0.2 means that 20% of the hydroxymethyl groups on cellulose have been oxidized to corresponding carboxylic acid groups and are thus susceptible for the subsequent grafting reactions. Therefore, the maximum grafting density corresponds to the situation where every fifth of the anhydroglucose units in cellulose contain a grafted propargylamine or an 11-azido-3,6,9-trioxaundecan-1-amine moiety. As a result, in the case of propargylamine, the completely grafted TEMPO-oxidized CNCs should contain 1.6% of nitrogen [14/(5 × 162 + 40)]. Similarly, the complete grafting of 11-azido-3,6,9-trioxaundecan-1-amine should produce modified CNCs with 5.5% nitrogen content (4 × 14/(5 × 162 + 217)]. However, the amount of nitrogen found in the precursors was 0.79% (CNC-PR) and 1.90% (CNC-AZ). This corresponds to grafting densities of ∼50% (CNC-PR) and ∼35% (CNC-AZ). Incomplete grafting is not totally surprising because the reactions were carried out under heterogeneous reaction conditions (aqueous suspensions). Efforts to further control the uniformity of these grafting reactions are underway in our laboratory by appropriately adjusting the grafting conditions.

Finally, it is important to mention here that the oxygen content was found to be elevated in the TEMPO-oxidized CNCs when compared to the CNCs, further supporting the occurrence of a successful oxidation reaction.

Thermal Analysis of TEMPO-Oxidized CNCs and Click Derivatives. In our efforts to investigate the thermal behavior of the formed click products we applied thermogravimetric analysis (TGA) for the determination of the thermal decomposition temperature. TGA analysis of the starting materials and the click product indicated significant changes in the decomposition profiles after the click reaction (Figure 4). The thermal degradation curves of the TEMPO-oxidized CNCs and both of the derivatives (CNC-AZ and CNC-PR) are almost identical while the click product (CNC-Click) seems to display two degradation profiles, that is, CNC-Click starts to degrade at temperatures similar (around 225 °C) to those of its precursors, and in addition, it shows a second thermal decomposition event at 325 °C.

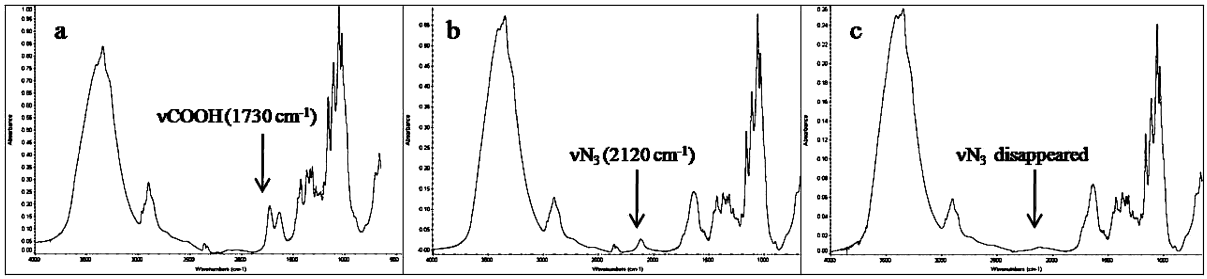

Figure 3. FTIR spectra of oxidized (TEMPO) cellulose nanocrystals (a), azido-derivatized cellulose nanocrystals (CNC-AZ) (b), and nanoplatelet gels (CNC-Click) (c).

Table 1. Carbon, Hydrogen, Oxygen, and Nitrogen Contents of the Cellulosic Samples

sample	% C	% H	% N	% O[a]
Tempo-ox. CNC	41.75	5.76	0.08	52.41
CNC	43.55	6.11	0.04	50.30
CNC-AZ	42.87	5.20	1.90	50.03
CNC-PR	43.20	5.29	0.79	50.72
CNC-Click	43.28	6.03	1.51	49.18

[a] O = 100% − C (%) − H (%) − N (%).

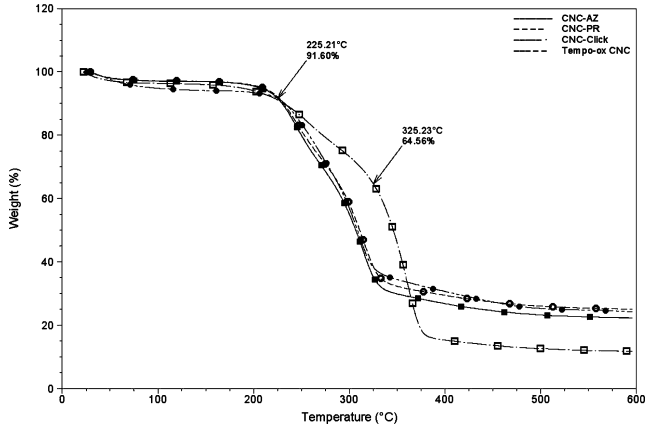

Figure 4. TGA curves of tempo-oxidized nanocrystals (circle markers), CNC-PR (open circle markers), CNC-AZ (square markers), and CNC-Click (open square markers).

GPC Analysis of Click Derivatives. The molecular weight distributions of both precursors (CNC-PR and CNC-AZ) and formed click product (CNC-Click) were investigated by size exclusion chromatography. Due to the insolubility of cellulosic samples in tetrahydrofuran (THF), all the hydroxyl groups on them were benzoylated prior to the analysis. To achieve a high degree of benzoylation, the reactions were carried out in ionic liquid, 1-allyl-3-methylimidazolium chloride ([Amim]Cl), which is known to be able to dissolve cellulosic materials. As expected, the molecular weight of the click product is considerably higher than those of the starting materials, indicating that the linking (Huisgen) reaction has occurred (Figure 5). As can be seen from Table 2, CNC-Click showed an approximately 5- to 6-fold increase in weight average molecular weight (M_w) when compared to its percursors (CNC-PR and CNC-AZ). Moreover, the significantly elevated polydispersity (PD; M_w/M_n) value of CNC-Click is characteristic for polydisperse materials. However, one needs to be aware of the limitations of gel permeation chromatography and the relative nature of our measurements as imposed by the use of polystyrene standards and their dissimilar nature with the benzoylated cellulosics examined. The use of absolute light scattering measurements is currently under consideration in our laboratory.

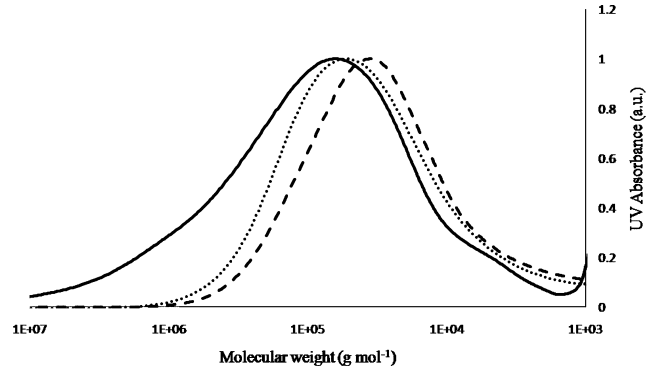

Figure 5. Gel permeation chromatograms of CNC precursors (CNC-PR, dotted line; CNC-AZ, dashed line) and cellulose nanoplatelet gel (CNC-Click, solid line).

Table 2. Molecular Weight Distributions of Starting Precursors (CNC-PR and CNC-AZ) and Click Product (CNC-Click)

sample	M_w (1×10^3 g mol^{-1})	polydispersity (PD)
CNC-PR	72	3.5
CNC-AZ	53	3.4
CNC-Click	335	12.6

TEM Analysis of TEMPO-Oxidized CNCs and Click Derivatives. An electron micrograph of the Click product is shown in Figure 6. As anticipated, the TEM image of the cross-linked CNCs revealed significantly larger particles being present than those obtained from the initial CNCs or the precursors used (approximately 10−20 nm in width and about 100−200 nm in length). It is apparent that the cycloaddition linking reaction has packed the crystals in an organized manner since the rectangular shape of the starting CNCs was retained.

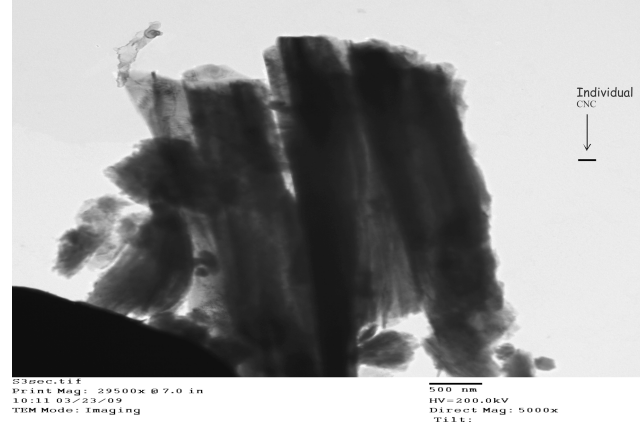

Figure 6. TEM image of cellulose nanoplatelet gel (CNC-Click). Scale bar 500 nm.

In accordance with our working hypothesis, the click chemistry locks into place the cellulose nanocrystals in a uniform vertical arrangement creating the observed vertical arrays. One possible explanation for the formation of these regular arrays may be the fact that self-assembly forces, operating between individual hydrated functionalized Click precursor nanocrystals, bring the hydrated nanocrystals together. In fact, the liquid crystalline properties of cellulose nanocrystals are well-known and documented.[40,41] They are then locked into place once the azide and the alkyne moieties are at close proximity. Current work in our laboratory aims to further explore the concentration effects of the click precursors prior to forming the nanoplatelet gels to shed more light and elucidate the stated hypothesis.

Interestingly, the resulting linked nanocrystals have not grown in one dimension as one would have anticipated from considering the activated C-6 positions (figure 6).

A minor degree of linking was found to occur, most likely, via the chain ends of the crystals causing growth in another dimension. This becomes apparent when one compares the size of the individual starting CNCs, shown as an insertion in Figure 6, to the resulting "tower"-like structures for the CNC-Click. The observed lateral linking is not totally surprising when one consider the chemistry of the oxidative treatment of the starting CNCs. In addition to oxidizing the surface hydromethyl groups, TEMPO-mediated oxidation may also introduce carboxylic groups to the reducing ends of the CNCs.[42–44] Therefore, the oxidized reducing end groups can become reactive toward the derivatization conditions that were used to form the alkyne and azido bearing precursors. Subsequently, the modified reducing end groups can also react under the click chemistry conditions, resulting in the multidimensional but rather regular growth observed in the TEM image of Figure 6. Additional control in the proposed linking chemistry is currently explored in our laboratory by the use of aldehyde blocking groups prior to the TEMPO oxidative activation.

Conclusions

Click chemistry has been utilized for the preparation of new gel-like cellulose nanomaterials. The primary hydroxyl groups in cellulose nanocrystals were first selectively activated by their conversion to carboxylic acids. These regularly spaced surface functionalities were further used as reactive sites for amidation reactions, providing the essential precursors to click chemistry. A TEM image of the produced materials showed evidence of the crystals being packed in an organized manner.

Acknowledgment. The authors would like to thank the College of Natural Resources at NCSU for the award of the Hofmann Fellowship to I.F., which made graduate studies possible.

References and Notes

(1) Heinze, T.; Liebert, T. *Prog. Polym. Sci.* **2001**, *26*, 1689–1762.
(2) Klemm, D. K.; Heublein, B.; Fink, H. P.; Bohn, A. *Angew. Chem., Int. Ed.* **2005**, *44*, 3358–3393.
(3) Huang, J.; Kunitake, T. *J. Am. Chem. Soc.* **2000**, *125*, 11834–11835.
(4) Liebert, T.; Hornig, S.; Hesse, S.; Heinze, T. *J. Am. Chem. Soc.* **2005**, *127*, 10484–10485.
(5) Huang, J.; Ichinose, I.; Kunitake, T. *Angew. Chem., Int. Ed.* **2006**, *118*, 2949–2952.
(6) Hoffmann, B.; Bernet, B.; Vasella, A. *Helv. Chim. Acta* **2002**, *85*, 265–287.
(7) Gallos, J. K.; Koumbis, A. E. *Curr. Org. Chem.* **2003**, *7*, 397–426.
(8) Huisgen, R. *Proc. Chem. Soc.* **1960**, 357–369.
(9) Tornøe, C. W.; Christensen, C.; Meldal, M. *J. Org. Chem.* **2002**, *67*, 3057–3064.
(10) Rostovtsev, V. V.; Green, L. G.; Fokin, V. V.; Sharpless, K. B. *Angew. Chem., Int. Ed.* **2002**, *41*, 2596–2599.
(11) Lewis, W. G.; Green, L. G.; Grynszpan, F.; Radic, Z.; Carlier, P. R.; Taylor, P.; Finn, M. G.; Sharpless, K. B. *Angew. Chem.* **2002**, *114*, 1095–1099.
(12) Lewis, W. G.; Green, L. G.; Grynszpan, F.; Radic, Z.; Carlier, P. R.; Taylor, P.; Green, M. G.; Fokin, V. V.; Sharpless, K. B. *Angew. Chem., Int. Ed.* **2002**, *41*, 1053–1057.
(13) Kolb, H. C.; Finn, M. G.; Sharpless, K. B. *Angew. Chem.* **2001**, *113*, 2056–2075.
(14) Iha, R. K.; Wooley, K. L.; Nyström, A. M.; Burke, D. J.; Kade, M. J.; Hawker, G. J. *Chem. Rev.* **2009**, *109*, 5620–5686.
(15) Huisgen, R. *Pure Appl. Chem.* **1989**, *61*, 613–628.
(16) Kolb, H. C.; Finn, M. G.; Sharpless, K. B. *Angew. Chem., Int. Ed.* **2001**, *40*, 2004–2021.
(17) Wu, P.; Feldman, A. K.; Nugent, A. K.; Hawker, C. J.; Scheel, A.; Voit, B.; Pyun, J.; Fréchet, J. M. J.; Sharpless, K. B.; Fokin, V. V. *Angew. Chem., Int. Ed.* **2004**, *43*, 3928–3932.
(18) Gupta, N.; Vestberg, R.; Malkoch, M.; Hikita, S. T.; Thibault, R. J.; Lingwood, M.; McCarney, E.; Han, S.; Clegg, O. D.; Hawker, C. J. *Polym. Prepr.* **2006**, *47*, 25–26.
(19) De Nooy, A. E.; Besemer, A. C.; van Bekkum, H. *Recl. Trav. Chim. Pays-Bas* **1994**, *113*, 165–166.
(20) Saito, T.; Isogai, A. *TAPPI J.* **2005**, *4*, 3–8.
(21) Tahiri, C.; Vignon, M. *Cellulose* **2000**, *7*, 177–188.
(22) Montanari, S.; Roumani, M.; Heux, L.; Vignon, M. *Macromolecules* **2005**, *38*, 1665–1671.
(23) Saito, T.; Shibata, I.; Isogai, A.; Suguri, N.; Sumikwa, N. *Carbohydr. Polym.* **2005**, *61*, 414–419.
(24) Saito, T.; Isogai, A. *Biomacromolecules* **2004**, *5*, 1983–1989.
(25) Araki, J.; Wada, M.; Kuga, S. *Langmuir* **2001**, *17*, 21–27.
(26) Crescenzi, V.; Cornelio, L.; Di Meo, C.; Nardecchia, S.; Lamanna, R. *Biomacromolecules* **2007**, *8*, 1844–1850.
(27) Hasegawa, T.; Umeda, M.; Numata, M.; Li, C.; Bae, A.-H.; Fujisawa, T.; Haraguchi, S.; Sakuraib, K.; Shinkaia, S. *Carbohydr. Res.* **2006**, *341*, 35–40.
(28) Ossipov, D. A.; Hilborn, J. *Macromolecules* **2006**, *39*, 1709–1718.
(29) Dìaz, D. D.; Rajagopal, K.; Strable, E.; Schneider, J.; Finn, M. G. *J. Am. Chem. Soc.* **2006**, *128*, 6056–6057.
(30) Liebert, T.; Hänsch, C.; Heinze, T. *Macromol. Rapid Commun.* **2006**, *27*, 208–213.
(31) Hafrén, J.; Zou, W.; Córdova, A. *Macromol. Rapid Commun.* **2006**, *27*, 1362–1366.
(32) Araki, J.; Wada, M.; Kuga, S.; Okano, T. *J. Wood Sci.* **1999**, *45*, 258–261.
(33) Araki, J.; Wada, M.; Kuga, S.; Okano, T. *Colloids Surf., A* **1998**, *142*, 75–82.
(34) Xie, H.; King, A.; Kilpelainen, I.; Granstrom, M.; Argyropoulos, D. S. *Biomacromolecules* **2007**, *8*, 3740–3748.
(35) Habibi, Y.; Chanzy, H.; Vignon, M. R. *Cellulose* **2006**, *13*, 679–687.
(36) Da Silva Perez, D.; Montanari, S.; Vignon, M. R. *Biomacromolecules* **2003**, *4*, 1417–1425.
(37) Saito, T.; Nishiyama, Y.; Putaux, J. L.; Vignon, M.; Isogai, A. *Biomacromolecules* **2006**, *7*, 1687–1691.
(38) Fan, L. T.; Gharpuray, M. M.; Lee, Y.-H. *Biotechnology Monographs*; Springer-Verlag: Berlin, 1987; p 76.
(39) Leppänen, K.; Andersson, S.; Torkkeli, M.; Knaapila, M.; Kotelnikova, N.; Serimaa, R. *Cellulose* **2009**, *16*, 999–1015.
(40) Beck-Candanedo, S.; Roman, M.; Gray, D. G. *Biomacromoleules* **2005**, *6*, 1048–1054.
(41) Wang, N.; Ding, E.; Cheng, R. *Langmuir* **2008**, *24*, 5–8.
(42) Shibata, I.; Isogai, A. *Cellulose* **2003**, *10*, 151–158.
(43) Ibert, M.; Marsais, F.; Merbouh, N. *Carbohydr. Res.* **2002**, *337*, 1059–1063.
(44) Kato, Y.; Matsuo, R.; Isogai, A. *Carbohydr. Polym.* **2003**, *51*, 69–75.

BM1000247